Environmental Science & Technology

pubs.acs.org/est

Article

Mechanisms of Uptake and Translocation of Thallium in *Brassica* Vegetables: An X-ray Fluorescence Microspectroscopic Investigation

Amelia Corzo-Remigio, Hugh H. Harris, Clinton J. Kidman, Philip Nti Nkrumah, Lachlan W. Casey, David J. Paterson, Mansour Edraki, and Antony van der Ent*

Cite This: *Environ. Sci. Technol.* 2024, 58, 2373−2383

Read Online

ACCESS | Metrics & More | Article Recommendations | Supporting Information

ABSTRACT: Most nonoccupational human exposure to thallium (Tl) occurs via consumption of contaminated food crops. *Brassica* cultivars are common crops that can accumulate more than 500 μg Tl g^{-1}. Knowledge of Tl uptake and translocation mechanisms in *Brassica* cultivars is fundamental to developing methods to inhibit Tl uptake or conversely for potential use in phytoremediation of polluted soils. *Brassica* cultivars (25 in total) were subjected to Tl dosing to screen for Tl accumulation. Seven high Tl-accumulating varieties were selected for follow-up Tl dosing experiments. The highest Tl accumulating *Brassica* cultivars were analyzed by synchrotron-based micro-X-ray fluorescence to investigate the Tl distribution and synchrotron-based X-ray absorption near-edge structure spectroscopy (XANES) to unravel Tl chemical speciation. The cultivars exhibited different Tl tolerance and accumulation patterns with some reaching up to 8300 μg Tl g^{-1}. The translocation factors for all the cultivars were >1 with *Brassica oleracea* var. *acephala* (kale) having the highest translocation factor of 167. In this cultivar, Tl is preferentially localized in the venules toward the apex and along the foliar margins and in minute hot spots in the leaf blade. This study revealed through scanning electron microscopy and X-ray fluorescence analysis that highly Tl-enriched crystals occur in the stoma openings of the leaves. The finding is further validated by XANES spectra that show that Tl(I) dominates in the aqueous as well as in the solid form. The high accumulation of Tl in these *Brassica* crops has important implications for food safety and results of this study help to understand the mechanisms of Tl uptake and translocation in these crops.

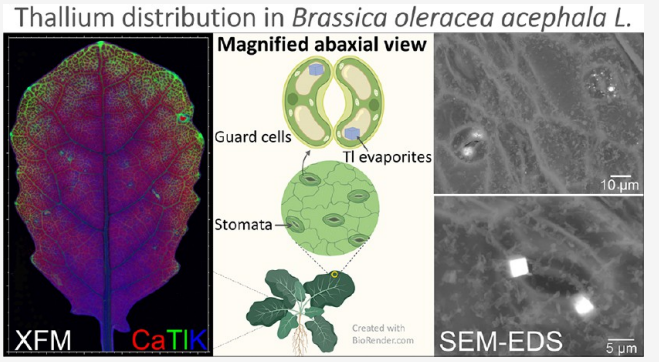

KEYWORDS: *Brassicas, bioconcentrations, health risk, phytoextraction, thallium*

INTRODUCTION

Thallium (Tl) is more toxic to mammals than arsenic (As), cadmium (Cd), mercury (Hg), or lead (Pb).[1] It is listed among the US Environmental Protection Agency's 13 priority pollutant metals.[2] Thallium occurs in the environment at very low concentrations, with an average crustal abundance of ~0.8 μg Tl g^{-1}.[3] However, geochemically anomalous areas and sites in the vicinity of base metal mines can have elevated Tl concentrations in the soil, e.g., 185 μg Tl g^{-1} in top soils at the Pollone Mine, Italy,[4] a maximum of 280 μg Tl g^{-1} in the bottom soils of the Jas Roux site, France,[5] 124 μg Tl g^{-1} at the Lanmuchang deposit in Guizhou Province, China,[6,7] and up to 18,000 μg Tl g^{-1} at the Allchar outcrop, North Macedonia.[8,9] Thallium occurs in two oxidation states in geochemical environments as Tl(I) and Tl(III), with the latter being 50,000-fold more toxic to phytoplanktons (unicellular algae, *Chlorella* sp.).[10]

Thallium is not essential for living organisms,[11] although it is readily taken up from soil by plants because it is generally present as the thermodynamically stable monovalent ion, with chemical properties similar to potassium (K).[12] In plants, Tl^+ is transported as the hydrated ion through K^+- and Na^+-selective channels.[13] A recent study on *Arabidopsis thaliana* reported that Tl interferes in K-dependent processes, inhibits photosynthetic activity, and enhances oxidative stress.[14] In *Dittrichia* plants exposed to 100 μM Tl, oxidative stress was observed as well as a decline of some nutrients (Fe, Mg, and K).[15] A study on *Sinapsis alba* (white mustard) showed that Tl tolerance decreased in higher Tl treatments, with evident effects on growth inhibition, oxidation of pigments, and a decline in photosystem core proteins.[16] Of all the nonessential trace elements, Tl has some of the highest bioaccumulation coefficients among plants, with high values reported in members of the Brassicaceae family.[17] The vegetable kale (*Brassica oleracea* var. *capitata*) and green cabbage (*Brassica*

Received: October 11, 2023
Revised: December 21, 2023
Accepted: December 22, 2023
Published: January 25, 2024

oleracea) accumulated >300 μg Tl g^{-1} when growing in soils with <70 μg Tl g^{-1}.[6,18,19] The Brassicaceae contains species that have been reported to accumulate Tl in edible parts and are commonly used as food crops (e.g., mustard, broccoli, Brussel sprouts, cabbage, cauliflower, and kale).[20−24] This suggests that Tl toxicity from vegetable consumption can easily occur. The World Health Organization set a maximum value of Tl in diet at 0.18 μg/kg body weight per day.[25] Exposure to, or consumption of, Tl can cause adverse health effects, including gastroenteritis, polyneuropathy, and alopecia, which can ultimately lead to death.[26]

Several *Brassica* crops have been studied for their ability to accumulate metal(loid)s and potential to remediate soils, e.g., *Brassica napus*[27] and *Brassica oleracea* var. *capitata*.[28] Indian mustard (*Brassica juncea*) is one of the most geographically distributed Brassicaceae crops and has been identified to withstand high Tl concentrations, with 3-fold potential benefits: (i) plant-based extraction of metals with economic value (phytomining) or of environmental concern, such as Tl, (ii) sustainable soil management, and (iii) use in bioprospecting during exploration for ore deposits. Plants grown in contaminated soil can contain ∼500 μg Tl g^{-1} and with an estimated biomass of 15 t ha^{-1} can yield a crop containing ∼7.5 kg Tl/ha/harvest.[21] Thallium hyperaccumulation in plants occurs in nature and is recognized in plants with in excess of 100 μg g^{-1} in above ground tissues,[29] although only six species have been reported so far. Two belong to the Brassicacea family, *Biscutella laevigata* (up to 32,700 μg Tl g^{-1} in their leaves)[30] and *Iberis intermedia* (up to 4000 μg Tl g^{-1}),[31] one to the Caryophyllaceae family, *Silene latifolia* (up to 35,700 μg Tl g^{-1}),[32] and three other are *Viola* taxa from the Violaceae family (*Viola tricolor* subsp. *macedonica*, *Viola allcharensis*, and *Viola arsenica*) with up to 58,900 μg Tl g^{-1}.[9]

Despite the human health risk of consuming Brassicaceae crops grown in Tl-contaminated soils, there is a paucity of studies on the chemical speciation and compartmentation of Tl in these crops, given the extreme toxicity of Tl(III) compared to Tl(I). Chemical speciation of Tl in *I. intermedia*, a Tl hyperaccumulator plant, has been studied to date using hyphenated chromatography methods[33] and synchrotron spectroscopy.[12] Synchrotron-based micro-X-ray fluorescence (μXRF) can shed light on the distribution of elements within plant tissues and cells, while synchrotron-based X-ray absorption near-edge structure spectroscopy (XANES) allows the understanding of the molecular forms and bonding of elements based on their wavelength and energy without using destructive sample preparation, which in plants might affect the elemental distribution and oxidation state of Tl.[34]

The aims of this study were (i) to compare Tl accumulation and tolerance in 25 cultivars of *Brassica* crops: *Brassica oleracea*, *Brassica juncea*, and *Brassica rapa* (*B. rapa*); (ii) to unravel Tl spatial distribution in *Brassica* crops with higher Tl uptake; and (iii) to elucidate Tl speciation in *Brassica* crops. Laboratory-based μXRF and synchrotron-based μXRF were used for the elemental distribution in *Brassica* leaves. Synchrotron-based XANES spectroscopy was used for Tl speciation analysis. This information can be used to better understand the ecotoxicology of these edible crops and to limit uptake of edible crops or conversely exploit the potential of these cultivars for remediation of Tl-polluted soils.

MATERIALS AND METHODS

Plant Culture Conditions. Seeds from 25 *Brassica* species and cultivars (Table S1) were germinated over 7 days in plastic trays (44 × 33 × 7 cm) filled with a mixture of a perlite:vermiculite (1:1, v:v) substrate. Seeds were sown 1 cm deep and 2 cm apart from each other and watered accordingly to water capacity. The growth chamber conditions were a 12/12 h light/dark cycle, using high-intensity photosynthetically active radiation (PAR) LED lights (Valoya model B200, Helsinki, Finland) at a photosynthetic photon flux density of 350 μmol m^{-2} s^{-1}, and a 26/20 °C day/night temperature regime. Five seedlings from each cultivar were then transferred to hydroponic cultures after the cotyledons had fully emerged. The hydroponics experiment was conducted in a temperature-controlled room with four containers (11 × 30 × 40 cm; capacity, ∼12 L). The solutions were aerated with air-stone diffusers at the base of each container. For experiment 1, on the 11th day, the nutrient solution was spiked with thallium(I)nitrate to make 7.5 μM Tl in a modified 1/2 strength Hoagland's solution. This 1/2 strength-modified Hoagland's formulation was prepared with K (3 mM as KNO_3), Ca (2 mM as $Ca(NO_3)_2{\cdot}4H_2O$), P (1 mM as $NH_4H_2PO_4$), N (8 mM as KNO_3, $Ca(NO_3)_2{\cdot}4H_2O$, and $NH_4H_2PO_4$), Mg (0.5 mM as $MgSO_4{\cdot}7H_2O$), Fe (40 μM as Fe(K)-HBED), Cl (1 μM as KCl), B (25 μM as H_3BO_3), Mn (2 μM as $MnSO_4{\cdot}4H_2O$), Zn (2 μM as $ZnSO_4{\cdot}7H_2O$), Cu (0.1 μM $CuSO_4{\cdot}5H_2O$), Mo (0.1 μM as $Na_2MoO_4{\cdot}2\ H_2O$), and 2 mM MES (2-(*N*-morpholino)ethanesulfonic acid) buffer adjusted to pH 5.5 with KOH.[35] After 11 days of exposure to Tl-spiked nutrient solution, leaves from each cultivar were imaged with laboratory-based μXRF analysis (Figure S1). *Brassica oleracea* cultivars with high Tl in their leaves (IDs 6, 9, 10, 11, 13, 15, and 16) were then selected for experiment 2 (Figure S2). The seven selected cultivars were germinated and grown in control nutrient solution for 11 days and then exposed to different levels of Tl (0, 1, 2.5, and 5 μM Tl). Some *Brassica oleracea* cultivars (IDs 6, 10, and 11) grown in 5 μM Tl (experiment 2) were transported to the Australian Synchrotron for XFM, and the remainder was harvested after 11 days of Tl exposure. Additionally, *Brassica oleracea* cultivars (IDs 10 and 11) grown in 7.5 μM Tl (following protocols of experiment 1) were transported to the Australian Synchrotron for X-ray absorption spectroscopy (XAS) analysis on bulk tissue samples.

Chemical Analysis of Plant Tissues. Harvested plant samples were thoroughly washed with distilled water and oven-dried for 72 h at 40 °C. Plant samples were homogenized and weighed to 100 ± 5 mg in 6 mL polypropylene tubes for predigestion using 2 mL HNO_3 (70%) for 24 h before digestion in a block heater (Thermo Scientific digital dry bath) for a 2 h program (1 h at 70 °C followed by 1 h at 125 °C). Ultrapure water (Millipore, 18.2 MΩ·cm at 25 °C) was added to the digested samples to make to 10 mL volume for elemental analysis using a Thermo Scientific iCAP 7400 inductively coupled plasma-atomic emission spectroscopy (ICP-AES) instrument. Either radial or axial mode was used depending on the approximate element concentrations in the solution. Matrix-based interferences were compensated using yttrium as in-line internal addition standardization. Quality controls included certified reference solution (Sigma-Aldrich Periodic Table Mix 1 for ICP TraceCERT, 33 elements, 10 mg

https://doi.org/10.1021/acs.est.3c08113
Environ. Sci. Technol. 2024, 58, 2373−2383

L^{-1} in HNO_3 70%, v/v), standard reference material (NIST Apple Leaves1515) treated as samples, and matrix blanks.

Scanning Electron Microscopy with Energy-Dispersive X-ray Spectroscopy (SEM-EDS). Small leaflet fragments were excised from the plant with a razor blade and immediately shock-frozen by quickly pressing against a solid block of stainless steel with a high thermal mass (2 kg) that was cooled by liquid nitrogen (−196 °C). Subsequently, the whole block (with samples in thermal contact) was moved into the vacuum chamber of a lyophilizer (Thermoline) and immediately pumped down. Vacuum (0.004 mbar) was achieved in <5 min, which ensured thermal insulation and ensured that the metal block remained cold and very slowly warmed to the set temperature of the lyophilizer (−85 °C). After 48 h, freeze-drying was progressed in increments of 5 °C and for another 24 h to room temperature (a total of 72 h). The samples were then stored in a box with silica gel, mounted on stubs, sputter-coated with carbon, and analyzed using scanning electron microscopy with energy-dispersive X-ray spectroscopy (SEM-EDS, Hitachi SU3500), at 100−3000× magnification at 15−20 kV, as described previously.[36]

Laboratory-Based Micro-X-ray Fluorescence (μXRF) Elemental Mapping. The University of Queensland (UQ) micro-X-ray fluorescence spectroscopy (μXRF) facility is a custom-built system assembled by IXRF Systems (TX, USA), which has two 50 kV−1000 μA sources fitted with polycapillary focusing optics. We used the microfocus Mo-target tube that produces 17.4 keV X-rays (flux of 2.2×10^8 ph s^{-1}) focusing to 25 μm. The fresh hydrated specimens belonging to the 25 *Brassica* cultivars were mounted between two sheets of Ultralene thin films (6 μm thick) stretched over a Perspex frame magnetically attached to the $x-y$ motion stage at atmospheric temperature (∼20 °C) (Figure S1). The XRF spectra were acquired in mapping mode using the instrument control package, Iridium (IXRF Systems).

Synchrotron-Based Micro-X-ray Fluorescence (μXRF) Elemental Mapping. The XFM beamline of the Australian Synchrotron employs an in-vacuum undulator to produce a brilliant X-ray beam with a focus down to 1 μm. A double-crystal monochromator Si(111) and Kirkpatrick−Baez mirrors produce a monochromatic focused incident beam onto the sample.[37,38] The beamline is equipped with a Maia XRF detection system, which enables short per pixel dwell times (down to submilliseconds) and large pixel counts (up to megapixels) for high-definition elemental imaging.[39] The μXRF elemental mapping used an incident energy of 15.8 keV. Three *Brassica oleracea* var. *acephala* cultivars were transported to the synchrotron XFM beamline (*Brassica* IDs 6, 10, and 11). Tissues (roots, stem, petiole, and leaf) and cross sections were imaged mounted between two sheets of 4 μm thick Ultralene thin films in a tight sandwich to limit evaporation. These tissue samples were sectioned with a vibratome using a "dry knife" method to avoid elemental redistribution and losses and this approach has been extensively validated in previous experiments.[35,40] The radiation dose to which the hydrated plant specimens were subjected was much lower (<0.5 kGy) than the dose required (>4 kGy) to induce noticeable damage.[41]

Synchrotron-Based X-ray Absorption Near-Edge Structure Spectroscopy (XANES). Solid standards were prepared with $Tl(I)NO_3$ and $Tl(III)_2O_3$ by mixing into cellulose powder at a final concentration of 5 μg Tl g^{-1}, and approximately 60 mg of each mixture was compressed to yield 4 mm-diameter pellets. The aqueous standards were prepared from $Tl(I)(NO_3)_{(s)}$ or $Tl(III)(NO_3)_{3(s)}$ with ultrapure water (Millipore), 100 mM HEPES (4-(2-hydroxyethyl)-1-piperazineethanesulfonic acid), and 100 mM BICINE (*N*,*N*-bis(2-hydroxyethyl)glycine) buffers, depending on the pH, and then with the following ligands: citrate, glutathione, and acetate. The pH of the ligands was adjusted with 5 M NaOH and 35% HCl. The solutions were diluted to 5 mM $[Tl^{+/3+}]$, as follows: 5 mM $[Tl^+]$ in 100 mM HEPES, pH 8; 5 mM $[Tl^+]$ in 25 mM citrate in 100 mM HEPES, pH 7.5; 5 mM $[Tl^+]$ in 25 mM glutathione in 100 mM HEPES, pH 7.5; 5 mM $[Tl^{3+}]$ in 100 mM acetate, pH 4; 5 mM $[Tl^+]$ in 25 mM glutathione in 100 mM BICINE, pH 9. Glycerol was added to avoid ice crystal formation (final concentration, 33 v/v%) to each standard before loading into plastic cells sealed with Kapton tape and plunge freezing in liquid nitrogen. Two cultivars from *Brassica oleracea* var. *acephala* were transported to Melbourne (IDs 10 and 11), and fresh hydrated dissected samples were inserted into the same plastic holders as the aqueous standards prior to rapid freezing in liquid nitrogen. Data collection was conducted at the XAS beamline at the Australian Synchrotron with the samples and standards at ∼5 K with the aid of a pulsed He expansion cryostat with Kapton windows. The incident X-ray beam was monochromated with a pair of Si(111) crystals, and harmonic rejection was achieved using a Rh-coated mirror. The data were collected in the fluorescence mode using an 18-element solid-state HP-Ge detector (Mirion, France), and the X-ray energy was calibrated by simultaneously collecting the transmission spectrum of an elemental selenium foil downstream of the sample (first peak of the first derivative assumed to be 12,658 eV). The XAS data were interpreted with standard approaches using EXAFSPAK software. All data were energy-calibrated, background-corrected, and normalized. Each XANES spectrum was then fit with a linear combination of the spectra of the following standards: $Tl(III)_2O_3$ (solid), $Tl(I)NO_3$ (solid), 5 mM Tl^+ solution in 25 mM citrate in 100 mM HEPES, pH 7.5, and 5 mM Tl^+ solution in 25 mM glutathione in 100 mM BICINE, pH 9. The spectra of these standards were distinct from each other and sufficient together to generate satisfactory fits to the various sample spectra. Components with a linear combination fit fraction less than three times the estimated standard deviation for that parameter were excluded.

Statistical Analyses. Statistical analyses were performed using R version 4.2.0 with RStudio 2022.02.2 with a significance level of $p < 0.05$. The assumption of data normality was evaluated using the Shapiro−Wilk test, and the homogeneity of variances was tested with Levene's test. The test of normality failed; therefore, nonparametric tests were conducted. For the experiment 1, the significance of differences in biomass and Tl concentration in shoots across the 25 cultivars was evaluated by a Kruskal−Wallis test followed by Dunn's pairwise *post hoc* tests. For experiment 2, biomass was assessed by a Kruskal−Wallis test followed by Dunn's pairwise *post hoc* tests for the seven selected cultivars. The significance of differences in thallium concentration in shoots, across different levels of Tl in nutrient solution in experiment 2, was evaluated with the nonparametric Scheirer−Ray−Hare test, equivalent to two-way ANOVA, followed by Dunn's pairwise *post hoc* tests. To identify if these food crops behave as thallium hyperaccumulators, the 25 cultivars were compared using the translocation factor (ratio of the element concentration in shoots to the element concentration in roots).

https://doi.org/10.1021/acs.est.3c08113
Environ. Sci. Technol. 2024, 58, 2373−2383

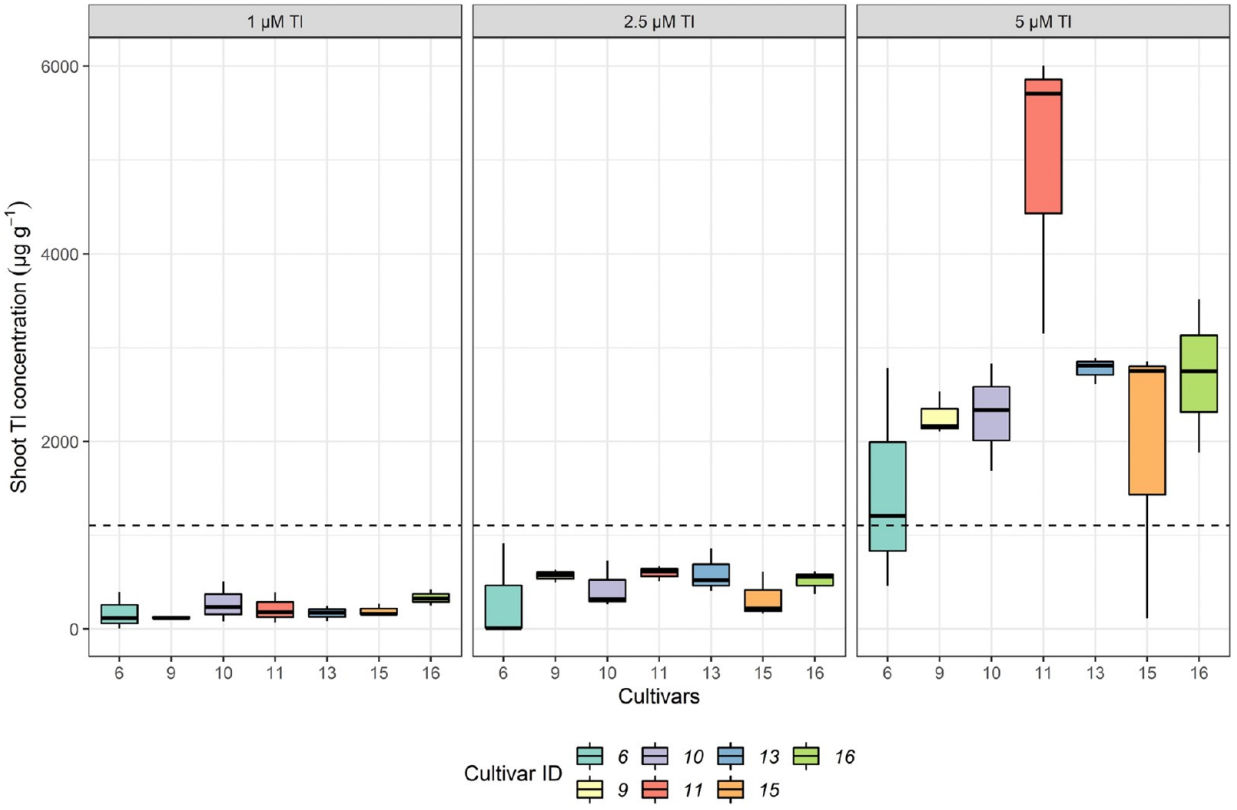

Figure 1. Thallium concentration graphs of seven selected *Brassica* cultivars grown in nutrient solution with different Tl concentrations (0, 1, 2.5, and 5 μM Tl). For each treatment, median values (line inside the box), 25−75% interquartile range boxes, and whiskers are displayed. The terminals of whiskers represent the lowest datum point still within 1.5 times the interquartile range of the lower quartile and the highest datum point still within 1.5 times the interquartile range of the upper quartile. Whiskers are not represented if the 25% interquartile was equal to the lowest datum point, or if the 75% interquartile was equal to the highest datum point (excluding outliers). Data were analyzed by the nonparametric Scheirer−Ray−Hare test followed by Dunn's test for the mean comparison ($p < 0.05$).

RESULTS

Plant Growth Performance in the Thallium Dosing Experiments. Total biomass results are presented in Figures S3a and S4 and Tables S1 and S2. For experiment 1, a Kruskal−Wallis test showed that there were significant differences in the biomass of the 25 cultivars subjected to 7.5 μM Tl ($H_{(24)} = 57.036$, $p = 0.00016$). The cultivars that had the highest biomass were cabbage and kale (*Brassica oleracea*), IDs 7, 8, 10, and 19, with median masses of 498, 1510, 632, and 410 mg, respectively, whereas the lowest biomass was recorded in mustard greens (*Brassica juncea*), IDs 23 and 24 with median masses of 35.7 and 26.3 mg per plant, respectively (Figure S3a and Table S1). For experiment 2, a Kruskal−Wallis test showed that there was a statistical difference in biomass across the seven selected cultivars (IDs 6, 9, 10, 11, 13, 15, and 16) across the different Tl treatments (0, 1, 2.5, and 5 μM Tl) ($H_{(3)} = 15.125$, $p = 0.0017$). The biomass of these cultivars decreased as the Tl concentrations in the nutrient solution increased (Figure S4). The cultivar ID 11 had the lowest biomass in the control solution (260 ± 103 mg per plant) and in the highest Tl treatment of 5 μM Tl (248 ± 32.7 mg per plant). In the 1 μM Tl treatment, all of the plants had slightly higher biomass compared to the other treatments, with the highest being cabbage, ID 6 (1930 ± 743 mg) (Figure S4 and Table S2).

Accumulation of Thallium in Roots and Shoots. Thallium accumulation in the *Brassica* cultivars is shown in Figure S3b, Figure 1, and Tables S1 and S2. For experiment 1, the uptake of Tl was statistically different across the 25 cultivars ($H_{(24)} = 58.686$, $p < 0.001$). *Brassica oleracea* varieties had the highest translocation factors compared to *B. juncea* and *B. rapa* subspecies. *Brassica oleracea* var. *acephala,* kale, ID 10 recorded a translocation factor of 167, which was >100-fold higher than that of *B. juncea* var. *rugosa*, mustard green, ID 22 (Table S1). For experiment 2, a Scheirer−Ray−Hare test showed a significant effect of Tl in nutrient solution for Tl accumulation in the *Brassica* selected cultivars ($H_{(3,140)} = 49.086$, $p < 0.001$), whereas the type of cultivar did not influence the Tl uptake ($H_{(6,140)} = 1.174$, $p = 0.978$). Thallium concentrations in the selected cultivars increased mirroring the concentration in the nutrient solution (Figure 1). The highest tissue Tl concentration was recorded at 5 μM Tl treatment in *B. oleracea* var. *acephala*, kale, ID 11, with a median of 5710 ± 905 μg Tl g^{-1}, and the lowest in *B. oleracea* capitata with 1210 ± 685 μg Tl g^{-1} growing in the 5 μM Tl treatment (Table S2).

Plant and Tissue-Level Distribution of Thallium Revealed by μXRF Analysis. Thallium spatial distributions in *Brassica* cultivar tissues and cross sections are shown in Figures 2−4 and Figures S1, S5, and S6. For comparison purposes, the macroelements calcium (Ca) and K distributions are included, as well as that of the micronutrient Zn. The μXRF spatial analysis confirmed high prevailing Tl concentrations in cultivars IDs 6, 9, 10, 11, 15, and 16 (Figure S1) and showed that Tl accumulation occurred mostly in the borders of the leaf, toward the apex. A closer view of old leaves of *Brassica* IDs 6 and 11 shows that Tl is distributed in a higher

https://doi.org/10.1021/acs.est.3c08113
Environ. Sci. Technol. 2024, 58, 2373−2383

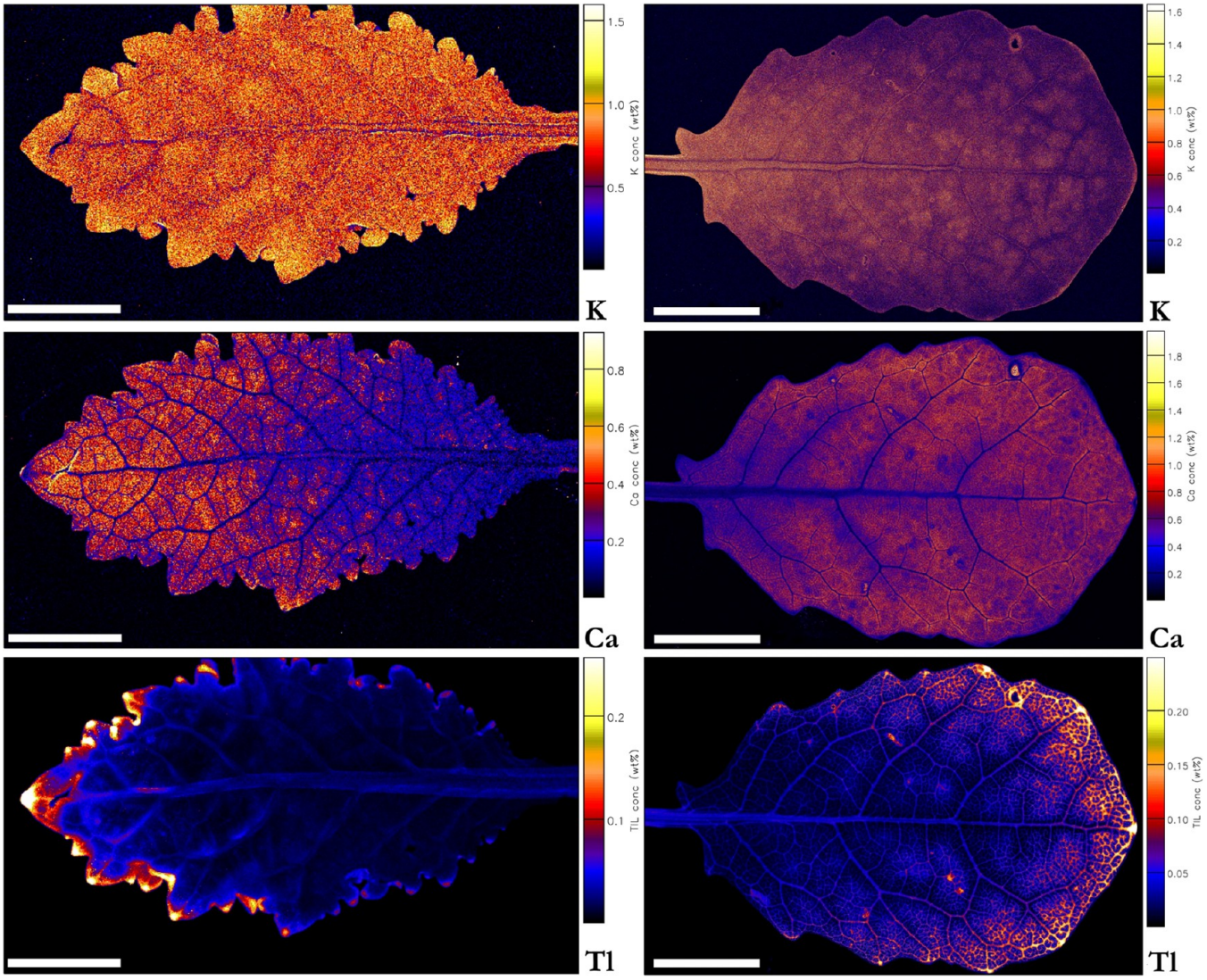

Figure 2. Synchrotron-based μXRF elemental maps of K, Ca, and Tl in leaves of *Brassica oleracea* var. *acephala*, kale, ID 10, midnight magic. On the left side of the image, a young leaf is shown, and on the right an old leaf. Scale bars denote 5 mm.

proportion in the margin protrusions closer to the apex. In both cultivars, Ca is distributed along the blade, with lower concentrations in the veins, midrib, and leaf base. Conversely, K is evenly distributed along the blade, although in a lower concentration (Figure S5). Young and old leaves of *Brassica* ID 10 display Tl accumulation toward the margin protrusions; in the old leaf, Tl is also present in the venules close to the margins (Figure 2). Calcium in *Brassica* ID 10 in the young leaf is higher in the blade close to the apex and lower close to the base leaf; however, Ca is higher in the young specimen. Potassium in the young leaf is evenly distributed along the blade, different from the old one in which K is lower. A high-resolution image of the margins of *Brassica* ID 10 shows a Tl enrichment in the venules (Figures 3 and 4). Calcium is low in the venules, whereas K is slightly higher in those areas (Figure 4). Cross sections of *Brassica* ID 10 showed Tl enrichment in the cambium and cortex of the stem and in the roots overall in the cortex (Figure S6). Notably, Tl enrichment in the stem and roots resembles that of K. Calcium in both the stem and roots is high in the cortex. The emerging lateral root is enriched in Tl, K, and Ca, whereas Zn is lower.

The SEM-BSE and EDS images of *Brassica oleracea* var. *acephala* abaxial leaflets are shown in Figure 5 and Figures S7 and S8, and the composition of major elements is summarized in Table S3. Major elements detected were O (range, 34.9−57.1 wt %), K (range, 13.9−35.1 wt %), Ca (6.6−17.6 wt %), P (range, 3.5−13.1 wt %), Mg (1.7−5.2 wt %), and S (range, 0.9−8.5 wt %). From the area EDS analysis, the spots 1, 3, 5, and 7 were located where Tl was below the detection limit to contrast with bright areas in the spots 2, 4, 6, and 8 where Tl is in the range from 0.3 to 1.7 wt % (Figure S7 and Table S3). Notably, Tl enrichment co-locates with Ca and S, which contrasts to K (Figure S8 and Table S3). A higher-magnification image of the abaxial old leaflets shows Tl-enriched crystals in the guard cells of the stomata (Figure 5).

Thallium Chemical Speciation in *Brassica oleracea* var. *acephala* Revealed by XANES Analysis. X-ray absorption spectra at the Tl L_{III} edge were collected from different sample locations of old and young leaves from the cultivars noted to have the highest Tl accumulation (IDs 10 and 11). The various sample spectra were fit with the spectra of a selection of standards as noted above. The standard set size was minimized by noting that the spectra for aqueous

https://doi.org/10.1021/acs.est.3c08113
Environ. Sci. Technol. 2024, 58, 2373−2383

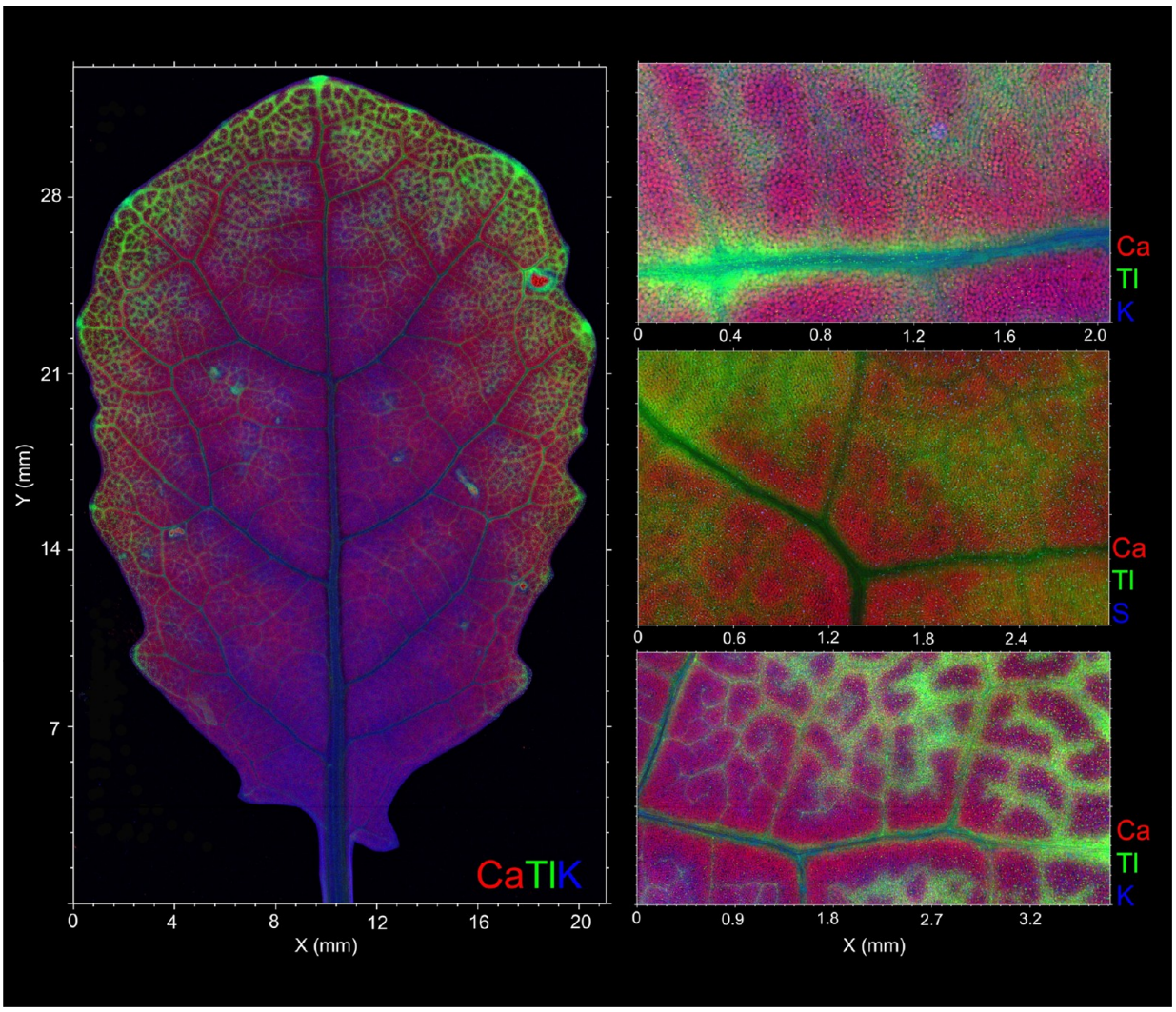

Figure 3. Synchrotron-based μXRF elemental maps of Ca, Tl, and K in an old leaf of *Brassica oleracea* var. *acephala*, kale, ID 10, midnight magic. On the left side of the image, an old whole leaf is shown, and on the high-resolution areas around the leaf veins.

solutions of Tl(I) in the presence of an excess of either glutathione or citrate at pH ∼7.4 were essentially indistinguishable (see trace D in Figure S9) and that the spectrum of $Tl(I)NO_{3(s)}$ was also indistinguishable from the spectrum of $Tl(I)_2SO_{4(s)}$ previously published by another group.[12] We noted that the spectra of the Tl(I) sulfate, chloride, and nitrate salts in aqueous solution as reported by Scheckel et al.[12] were all similar to each other and similar to our aqueous Tl(I) standard spectra and as such chose to use our spectrum (aqueous Tl(I) in excess citrate at pH ∼7.4) as a spectral model to represent "aqueous Tl(I)". A spectrum of aqueous Tl(I) in excess glutathione at pH ∼9 (Figure S9, trace B) was also included in the fits as it was distinct from the lower-pH aqueous Tl(I) spectrum, but we are unable to determine the exact nature of the Tl coordination in that solution (i.e., we do not know if Tl(I) is coordinated by a thiolate donor from glutathione or coordinated by just the carboxylates that are likely donors at lower pH, with a change in spectral features just reflecting a change in the protonation state of the complex). We chose our spectrum of $Tl(I)NO_{3(s)}$ to represent Tl(I) in a solid form, and the spectrum of this standard (Figure S9, trace C) is distinct from those of the aqueous spectra, with the first main peak appearing at ∼2 eV lower in energy. The spectrum of $Tl(III)_2O_{3(s)}$ was included in the linear combination fits and is unsurprisingly distinct from the spectra of the Tl(I) compounds. We were unable to collect reliable spectra of other Tl(III) compounds, but the quality of the fits that we obtain with the four standards that we chose, the similarity of the various Tl(III) spectra reported by Scheckel et al., and the fact that the thallium(III) oxide is only ever found as a minor component in the fits indicate that other Tl(III) contributions are not important in the context of these samples. Figure 6 shows the Tl XANES spectra that were collected from *Brassica* IDs 10 and 11 from different leaflet sections, and Table S4 shows the results of linear combination fits of the set of four spectral models to the respective plant spectra (see also Figures S10 and S11). In most cases, the fits reveal that the primary chemical form of Tl in the plant samples is a mixture of solid and aqueous forms of Tl(I), with occasional moderate contributions from the pH 9 GSH model and/or minor $Tl(III)_2O_{3(s)}$. The latter is never present at more than 5% in any of the sample fits, but given that its spectrum is very distinct from the other models, it may well be reliably identified in this analysis. The importance of the inclusion of the pH 9 GSH spectrum is unclear, especially because the

https://doi.org/10.1021/acs.est.3c08113
Environ. Sci. Technol. 2024, 58, 2373−2383

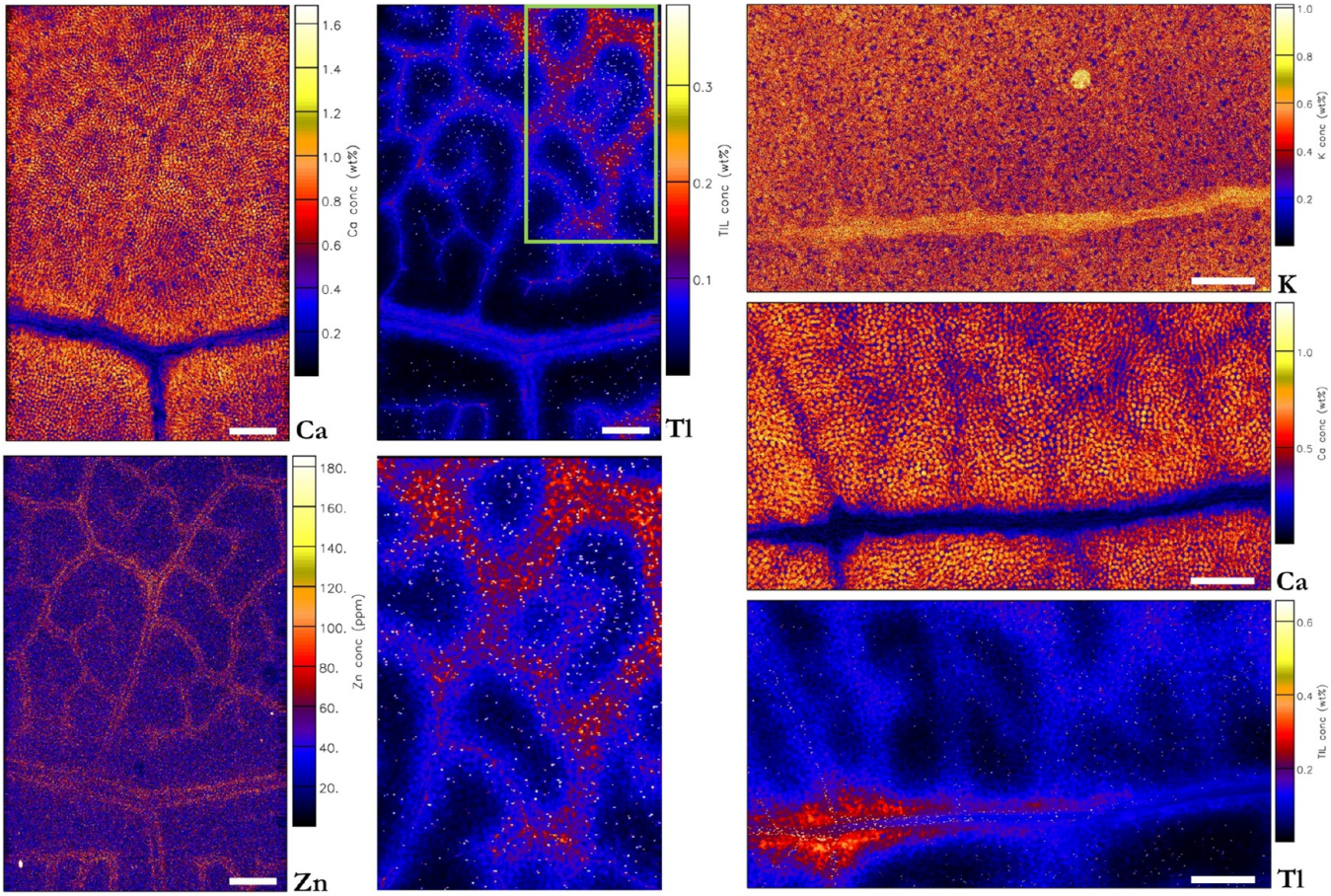

Figure 4. Synchrotron-based μXRF elemental maps of K, Ca, Zn, and Tl in old leaf veins of *Brassica oleracea* var. *acephala*, kale, ID 10, midnight magic. Scale bars denote 250 μm.

coordination environment in the standard is not well-characterized.

DISCUSSION

This study provides further information about Tl tolerance and (hyper)accumulation in 25 edible *Brassica* species/varieties by examining Tl distribution and speciation in the most tolerant cultivars. All of the cultivars subjected to 7.5 μM Tl exceeded the threshold for Tl hyperaccumulation of 100 μg g^{-1} foliar Tl.[29] The Brassicaceae family has most of the known metal hyperaccumulator plants.[42,43] Our study showed that crops belonging to *B. oleracea* (cabbage), *B. oleracea* var. *capitata* (cabbage), *B. oleracea* var. *acephala* (kale), and *Brassica oleracea* var. *italica* (broccoli) accumulated over 3000 μg Tl g^{-1} in shoots, while *B. juncea* (mustard greens) recorded lower concentrations, up to 1250 μg Tl g^{-1} (Table S1). There is consensus in previous research showing up to 30-fold higher Tl uptake of *B. oleracea* var. *acephala* (kale) compared to white cabbage (*B. oleracea* var. *capitata*).[44]

Green cabbage (*Brassica oleracea*) has one of the highest known Tl bioaccumulation factors (ratio of plant:soil) and translocation factors (ratio of shoot:root) with 1.35 and 2.92, respectively.[45] *Biscutella laevigata*, the strongest Tl hyperaccumulator known to date, was reported with a translocation factor of 19.4 ± 17.2.[46] Thallium can be easily transported through the food chain even from very low soil concentrations. For example, rape (*Brassica napus*) was reported to have ∼33 μg Tl g^{-1} in leaves whilst growing on soils with 0.4−40 μg Tl g^{-1}; as the seed of this plant is used for rape cake in cattle feed, it makes bioaccumulation and biomagnification possible through the food chain.[17]

The Tl-rich crystals observed in the scanning electron micrographs and in the X-ray fluorescence maps could be formed by guttation through hydathodes and stomata, as a result of an excess of Tl (Figure 5); this process was observed for Ni and Mn in hyperaccumulator plants growing in ultramafic soils.[47] The Tl-rich crystals are likely evaporites (salt deposits) that are left behind in the stoma openings. We hypothesize that Tl could be stored in guard cells of the stomata and transferred to other subsidiary cells, following the same pathway of K$^+$.[48] Thallium accumulation predominates around the foliar margins, where hydathode stomata secrete water. This process is likely similar to that of many halophytes expelling excess salts.[49]

The determination of the oxidation state of Tl and its distribution and detoxification in plants is fundamental to address the food safety risks, as one of the pathways to humans is through the food chain.[33] A study on Tl speciation using ion chromatography and inductively coupled plasma-mass spectroscopy (ICP-MS) focusing on *I. intermedia* reported that Tl was present in the reduced form Tl(I), and that it did not oxidize to Tl(III) in the plant.[33] This finding was later validated using XANES analysis, where Tl(I) in the aqueous form was found in the vascular system of *I. intermedia*.[12,34] In *Sinapis alba* (white mustard), XANES analysis reported spectra similar to aqueous Tl(I) and Tl(I)-acetate; S-coordinated

https://doi.org/10.1021/acs.est.3c08113
Environ. Sci. Technol. 2024, 58, 2373−2383

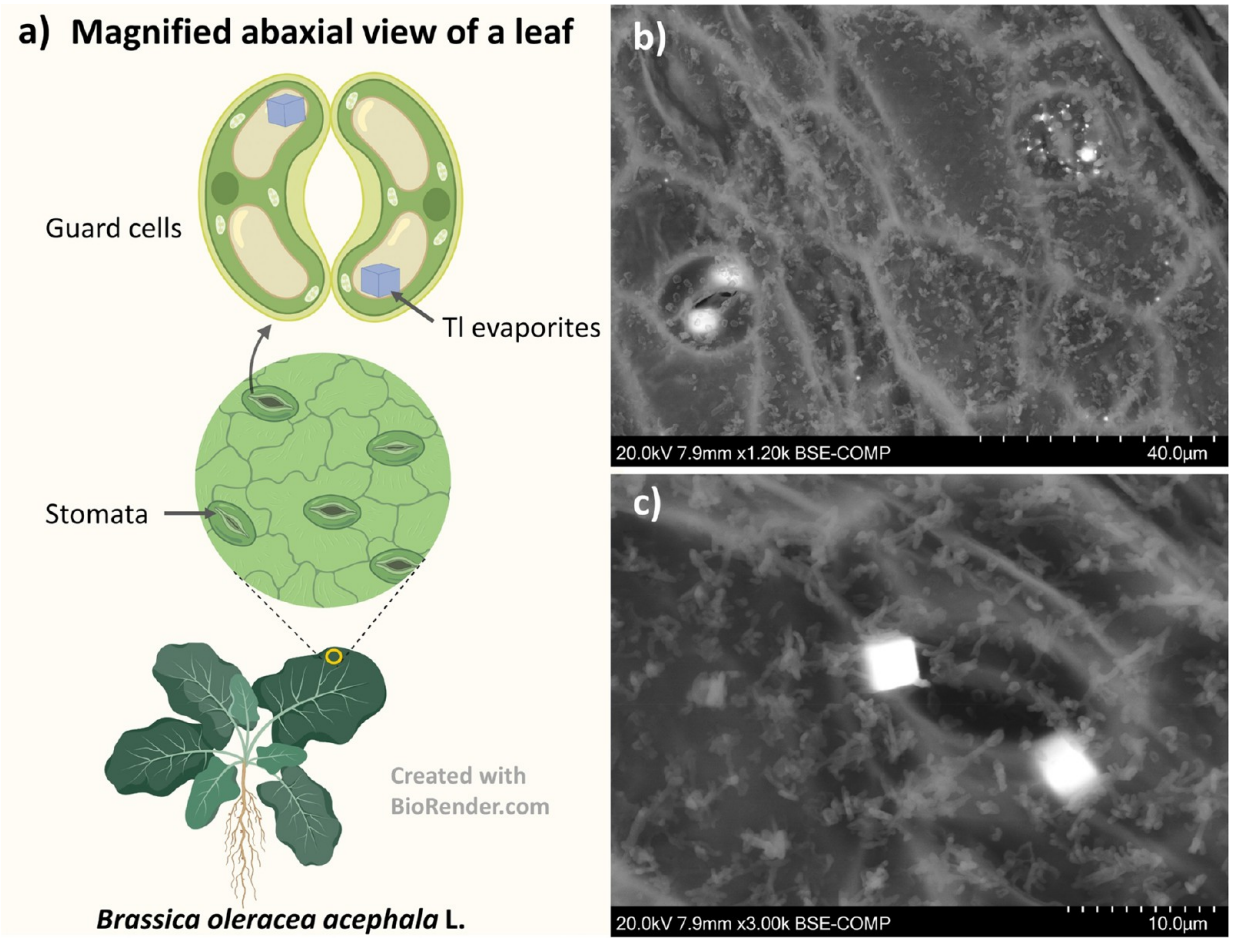

Figure 5. Scanning electron microscopy-backscattered electron (SEM-BSE) images of a freeze-dried *Brassica oleracea* var. *acephala*, kale, (midnight magic) leaf specimen from the 5 μM Tl treatment: (a) graphical representation of Tl crystallization in the stomata and guard cells of the specimen; (b) low-magnification image of the abaxial old leaflet with bright areas (Tl-enriched); (c) higher-magnification image of the abaxial leaflet area where Tl crystals can be observed.

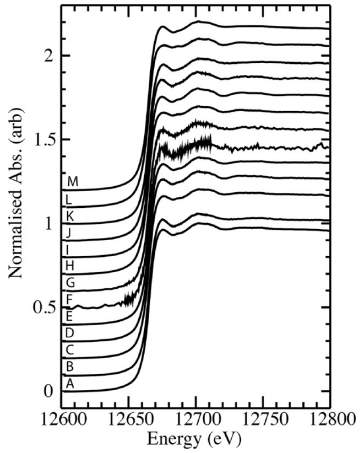

Figure 6. Tl L_{III}-edge X-ray absorption edge spectra of plant samples. (A) B10 old leaf, border; (B) B10 old leaf, center; (C) B10 old leaf, border; (D) B10 old leaf, border; (E) B10 old leaf, mush; (F) B10, root; (G) B10 young leaf, tip; (H) B11 old leaf, border; (I) B11 old leaf, center; (J) B11 old leaf, border; (K) B11 old leaf, border; (L), B11 old leaf, tip; (M) B10 old leaf, tip. B10 denotes *Brassica oleracea* var. *acephala*, kale, ID 10, midnight magic. B11 denotes *Brassica oleracea* var. *acephala*, kale, ID 11, Scotch (Borecole).

Tl(I) spectra were not related to the plant Tl spectra.[50] In our study, the Tl L_{III} edge XANES spectra of hydrated *Brassica* samples (ID 10 and ID 11 cultivars) showed that Tl(I) predominates in the aqueous as well as in the solid form (Table S4). This solid form was observed in Tl-enriched crystals in SEM-EDS analysis (Figure 5) and found in inclusions in the margins of fresh leaves (Figure 4). Minor contributions of Tl(III), less than 5%, were also identified in the ID 10 cultivar (Table S4). A similar result was reported in *S. alba* with approximately 10% of extracted Tl present as Tl(III) using high-performance liquid chromatography (HPLC) with ICP-MS analysis.[51] It has been hypothesized that Tl(III) in *S. alba* is present as an unstable compound that it is easily reduced to Tl(I).[52] Thallium(III) is very unstable in aqueous solution as the reduction potential of Tl(III) to Tl(I) requires only +1.26 V.[53] Oxidation of Tl(I) to Tl(III) might occur in small quantities in plants, and despite the higher toxicity of Tl(III), it forms more stable complexes with organic ligands (cysteine or glutathione), and does not interfere with K metabolism.[12,51]

Brassica crops are considered healthy superfoods, especially kale (*B. oleracea* var. *acephala*)[54], but there is a risk for Tl accumulation when grown in certain soils contaminated with Tl. Government regulations regarding Tl food safety and maximum permissible levels are scarce. In fact, Tl has not been

https://doi.org/10.1021/acs.est.3c08113
Environ. Sci. Technol. 2024, 58, 2373−2383

listed as a contaminant for food according to Australian regulations; only Pb has a maximum level of 0.3 $\mu g\ g^{-1}$ for *Brassica*.[55] The National Health and Medical Research Council did not include the reference value for Tl and other toxic elements such as As and Pb.[56] Additionally, Tl levels for ecological investigation in soils are not present in the Australian ecological risk assessment guideline NEPC.[57] Similarly, in other countries there is a lack of guidelines for Tl in soils and food stuffs, despite concerning research findings in e.g., China[45] and Korea.[58] In Canada, the Tl soil quality guideline for environmental health is 1 mg kg^{-1} considering soil and food ingestion for agriculture,[59] and in Germany, the Tl maximum permissible level for food stuffs is 0.5 mg kg^{-1}.[45] The European Food Safety Authority has been working toward developing a chemical food risk assessment for Tl and has highlighted the need of human toxicity studies as the release of Tl into the environment has increased as a consequence of industrial processes and contamination.[60]

The combination of many Brassicaceae as being active Tl bioaccumulators and food crops presents both environmental and human health risks. The results of this study help to better understand the mechanisms of Tl uptake and translocation in Brassicaceae crops, which is fundamental to developing effective methods to inhibit Tl uptake, or conversely, for potential use in phytoremediation aimed at extracting Tl from contaminated soils. Further studies involving comparative transcriptomics using *Brassica* cultivars contrasting in their Tl accumulation and tolerance can lead to the discovery of genes involved in enhanced root Tl uptake and tolerance mechanisms.

■ ASSOCIATED CONTENT

Supporting Information

The Supporting Information is available free of charge at https://pubs.acs.org/doi/10.1021/acs.est.3c08113.

Additional experimental details and results from the XFM, SEM-EDS, and XANES analysis (PDF)

■ AUTHOR INFORMATION

Corresponding Author

Antony van der Ent − *Centre for Mined Land Rehabilitation, Sustainable Minerals Institute, The University of Queensland, Brisbane 4072, Australia; Laboratory of Genetics, Wageningen University and Research, Wageningen 6708, The Netherlands;* orcid.org/0000-0003-0922-5065; Email: a.vanderent@uq.edu.au

Authors

Amelia Corzo-Remigio − *Centre for Water in the Minerals Industry, Sustainable Minerals Institute, The University of Queensland, Brisbane 4072, Australia;* orcid.org/0000-0003-3760-3350

Hugh H. Harris − *Department of Chemistry, The University of Adelaide, Adelaide 5005, Australia;* orcid.org/0000-0002-3472-8628

Clinton J. Kidman − *Department of Chemistry, The University of Adelaide, Adelaide 5005, Australia*

Philip Nti Nkrumah − *Centre for Mined Land Rehabilitation, Sustainable Minerals Institute, The University of Queensland, Brisbane 4072, Australia;* orcid.org/0000-0003-1437-4305

Lachlan W. Casey − *Centre for Microscopy and Microanalysis, The University of Queensland, Brisbane 4072, Australia*

David J. Paterson − *Australian Synchrotron (ANSTO), Clayton 3168, Australia;* orcid.org/0000-0003-0409-9012

Mansour Edraki − *Centre for Water in the Minerals Industry, Sustainable Minerals Institute, The University of Queensland, Brisbane 4072, Australia*

Complete contact information is available at: https://pubs.acs.org/10.1021/acs.est.3c08113

Author Contributions

A.C.-R. and A.V.D.E. designed and conducted the experiment. A.C.-R. collected the samples and undertook the chemical analysis of the samples. A.C.-R., P.N.N., L.W.C., H.H.H., and D.J.P. conducted the synchrotron experiments. A.C.-R., A.V.D.E., D.J.P., C.J.K., and H.H.H. processed the synchrotron XFM and XANES data. A.C.-R., H.H.H., S.J.P., M.E., D.J.P., and A.V.D.E. wrote the manuscript.

Funding

None declared.

Notes

The authors declare no competing financial interest.

■ ACKNOWLEDGMENTS

This research was undertaken on the X-ray Fluorescence Microscopy and X-ray Absorption Spectroscopy beamlines at the Australian Synchrotron, part of ANSTO. The microXRF analysis was undertaken at the Centre for Microscopy and Microanalysis (CMM) at the University of Queensland, Australia. We acknowledge support of Microscopy Australia at the Center for Microscopy and Microanalysis at the University of Queensland. We thank Enzo Lombi for providing XANES spectra of thallium compounds for comparison.

■ REFERENCES

(1) Lennartson, A. Toxic thallium. *Nat. Chem.* **2015**, *7* (7), 610−610.

(2) US EPA. *Code of Federal Regulation (40) Appendix A to Part 423—126 Priority Pollutants*. Agency, U E. P. Ed.; 2014.

(3) Kabata-Pendias, A.; Pendias, H. *Trace elements in soils and plants*; CRC Press, 2001.

(4) D'Orazio, M.; Campanella, B.; Bramanti, E.; Ghezzi, L.; Onor, M.; Vianello, G.; Vittori-Antisari, L.; Petrini, R. Thallium pollution in water, soils and plants from a past-mining site of Tuscany: sources, transfer processes and toxicity. *Journal of Geochemical Exploration* **2020**, *209*, No. 106434.

(5) Rose, J.; Chaurand, P.; Dentant, C.; Angeletti, B.; Borschneck, D.; Kieffer, I.; Proux, O.; Bonet, R.; Auffan, M.; Levard, C.; Fehlauer, T.; Collin, B.; Doelsch, E. Thallium long-term fate from rock-deposit to soil: the Jas Roux sulfosalt natural analogue. *ACS Earth and Space Chemistry* **2023**, *7* (10), 1848−1857.

(6) Xiao, T.; Guha, J.; Boyle, D.; Liu, C.-Q.; Zheng, B.; Wilson, G. C.; Rouleau, A.; Chen, J. Naturally occurring thallium: a hidden geoenvironmental health hazard? *Environ. Int.* **2004**, *30* (4), 501−507.

(7) Xiao, T.; Guha, J.; Boyle, D.; Liu, C.-Q.; Chen, J. Environmental concerns related to high thallium levels in soils and thallium uptake by plants in southwest Guizhou. *China. Sci. Total Environ.* **2004**, *318* (1), 223−244.

(8) Đorđević, T.; Drahota, P.; Kolitsch, U.; Majzlan, J.; Peřestá, M.; Kiefer, S.; Stöger-Pollach, M.; Tepe, N.; Hofmann, T.; Mikuš, T.; Tasev, G.; Serafimovski, T.; Boev, I.; Boev, B. Synergetic Tl and As retention in secondary minerals: an example of extreme arsenic and thallium pollution. *Appl. Geochem.* **2021**, *135*, No. 105114.

(9) Jakovljević, K.; Mišljenović, T.; Bačeva Andonovska, K.; Echevarria, G.; Baker, A. J. M.; Brueckner, D.; van der Ent, A. Thallium hyperaccumulation status of the violets of the Allchar arsenic−thallium deposit (North Macedonia) confirmed through synchrotron μXRF imaging. *Metallomics* **2023**, *15* (11), mfad063.
(10) Ralph, L.; Twiss, M. R. Comparative toxicity of thallium(I), thallium(III), and cadmium(II) to the unicellular alga *Chlorella* isolated from Lake Erie. *Bull. Environ. Contam. Toxicol.* **2002**, *68* (2), 261−268.
(11) Wiggenhauser, M.; Moore, R. E. T.; Wang, P.; Bienert, G. P.; Laursen, K. H.; Blotevogel, S. Stable isotope fractionation of metals and metalloids in plants: a review. *Front. Plant Sci.* **2022**, *13*, No. 840941.
(12) Scheckel, K. G.; Lombi, E.; Rock, S. A.; McLaughlin, M. J. In vivo synchrotron study of thallium speciation and compartmentation in *Iberis intermedia*. *Environ. Sci. Technol.* **2004**, *38* (19), 5095−5100.
(13) Galván-Arzate, S.; Santamaría, A. Thallium toxicity. *Toxicol. Lett.* **1998**, *99* (1), 1−13.
(14) Chang, H. F.; Tseng, S. C.; Tang, M. T.; Hsiao, S. S. Y.; Lee, D. C.; Wang, S. L.; Yeh, K. C.Physiology and molecular basis of thallium toxicity and accumulation in *Arabidopsis thaliana* Available at SSRN **2022**, DOI: 10.2139/ssrn.4196841.
(15) Espinosa, F.; Ortega, A.; Espinosa-Vellarino, F. L.; Garrido, I. Effect of thallium(i) on growth, nutrient absorption, photosynthetic pigments, and antioxidant response of *Dittrichia* plants. *Antioxidants* **2023**, *12* (3), 678.
(16) Mazur, R.; Sadowska, M.; Kowalewska, Ł.; Abratowska, A.; Kalaji, H. M.; Mostowska, A.; Garstka, M.; Krasnodębska-Ostręga, B. Overlapping toxic effect of long term thallium exposure on white mustard (*Sinapis alba* L.) photosynthetic activity. *BMC Plant Biol.* **2016**, *16* (1), 191.
(17) Tremel, A.; Masson, P.; Garraud, H.; Donard, O. F. X.; Baize, D.; Mench, M. Thallium in French agrosystems—II. Concentration of thallium in field-grown rape and some other plant species. *Environ. Pollut.* **1997**, *97* (1), 161−168.
(18) Pavlíčková, J.; Zbíral, J.; Smatanová, M.; Habarta, P.; Houserová, P.; Kubáň, V. Uptake of thallium from artificially contaminated soils by kale (*Brassica oleracea* L., var. *acephala*). *Plant Soil Environ.* **2006**, *52*, 544−549.
(19) Xiao, T.; Guha, J. Environmental exposure of thallium and potential health risk in the areas of high natural concentrations of thallium: southwest Guizhou. *China. Chin. J. Geochem.* **2006**, *25* (1), 22−22.
(20) Vejvodová, K.; Vaněk, A.; Drábek, O.; Spasić, M. Understanding stable Tl isotopes in industrial processes and the environment: a review. *J. Environ. Manage.* **2022**, *315*, No. 115151.
(21) Rader, S. T.; Maier, R. M.; Barton, M. D.; Mazdab, F. K. Uptake and fractionation of thallium by *Brassica juncea* in a geogenic thallium-amended substrate. *Environ. Sci. Technol.* **2019**, *53* (5), 2441−2449.
(22) Xiao, X.; Zhou, W.; Guo, Z.; Peng, C.; Xu, R.; Zhang, Y.; Yang, Y. Thallium content in vegetables and derivation of threshold for safe food production in soil: a meta-analysis. *Sci. Total Environ.* **2024**, *912*, No. 168845.
(23) Jia, Y.; Xiao, T.; Zhou, G.; Ning, Z. Thallium at the interface of soil and green cabbage (*Brassica oleracea* L. *var. capitata* L.): soil−plant transfer and influencing factors. *Sci. Total Environ.* **2013**, *450*−*451*, 140−147.
(24) Liu, J.; Luo, X.; Wang, J.; Xiao, T.; Chen, D.; Sheng, G.; Yin, M.; Lippold, H.; Wang, C.; Chen, Y. Thallium contamination in arable soils and vegetables around a steel plant—a newly-found significant source of Tl pollution in South China. *Environ. Pollut.* **2017**, *224*, 445−453.
(25) World Health Organization. *Environmental Health Criteria 182: Thallium*. WHO, 1996. http://www.inchem.org/documents/ehc/ehc/ehc182.htm#SectionNumber:1.4.
(26) Xiao, T.; Yang, F.; Li, S.; Zheng, B.; Ning, Z. Thallium pollution in China: a geo-environmental perspective. *Sci. Total Environ.* **2012**, *421*−*422*, 51−58.
(27) Dhiman, S. S.; Selvaraj, C.; Li, J.; Singh, R.; Zhao, X.; Kim, D.; Kim, J. Y.; Kang, Y. C.; Lee, J.-K. Phytoremediation of metal-contaminated soils by the hyperaccumulator canola (*Brassica napus* L.) and the use of its biomass for ethanol production. *Fuel* **2016**, *183*, 107−114.
(28) Jia, Y.; Xiao, T.; Sun, J.; Ning, Z.; Xiao, E.; Lan, X.; Chen, Y. Calcium enhances thallium uptake in green cabbage (*Brassica oleracea* var. *capitata* L.). *Int. J. Environ. Res. Public Health* **2023**, *20* (1), 4.
(29) van der Ent, A.; Baker, A. J. M.; Reeves, R. D.; Pollard, A. J.; Schat, H. Hyperaccumulators of metal and metalloid trace elements: facts and fiction. *Plant Soil* **2013**, *362* (1), 319−334.
(30) Fellet, G.; Pošćić, F.; Casolo, V.; Marchiol, L. Metallophytes and thallium hyperaccumulation at the former Raibl lead/zinc mining site (Julian Alps, Italy). *Plant Biosystems - An International Journal Dealing with all Aspects of Plant Biology* **2012**, *146* (4), 1023−1036.
(31) LaCoste, C.; Robinson, B.; Brooks, R.; Anderson, C.; Chiarucci, A.; Leblanc, M. The phytoremediation potential of thallium-contaminated soils using *Iberis* and *Biscutella* species. *International Journal of Phytoremediation* **1999**, *1* (4), 327−338.
(32) Corzo Remigio, A.; Nkrumah, P. N.; Pošćić, F.; Edraki, M.; Baker, A. J. M.; van der Ent, A. Thallium accumulation and distribution in *Silene latifolia* (Caryophyllaceae) grown in hydroponics. *Plant Soil* **2022**, *480* (1), 213−226.
(33) Nolan, A.; Schaumlöffel, D.; Lombi, E.; Ouerdane, L.; Łobiński, R.; McLaughlin, M. Determination of Tl(I) and Tl(III) by IC-ICP-MS and application to Tl speciation analysis in the Tl hyper-accumulator plant *Iberis intermedia*. *J. Anal. At. Spectrom.* **2004**, *19* (6), 757−761.
(34) Scheckel, K. G.; Hamon, R.; Jassogne, L.; Rivers, M.; Lombi, E. Synchrotron X-ray absorption-edge computed microtomography imaging of thallium compartmentalization in *Iberis intermedia*. *Plant Soil* **2007**, *290* (1), 51−60.
(35) van der Zee, L.; Corzo Remigio, A.; Casey, L. W.; Purwadi, I.; Yamjabok, J.; van der Ent, A.; Kootstra, G.; Aarts, M. G. M. Quantification of spatial metal accumulation patterns in Noccaea caerulescens by X-ray fluorescence image processing for genetic studies. *Plant Methods* **2021**, *17* (1), 86.
(36) Corzo Remigio, A.; Edraki, M.; Baker, A. J. M.; van der Ent, A. Is the aquatic macrophyte *Crassula helmsii* a genuine copper hyperaccumulator? *Plant Soil* **2021**, *464* (1), 359−374.
(37) Paterson, D.; de Jonge, M. D.; Howard, D. L.; Lewis, W.; McKinlay, J.; Starritt, A.; Kusel, M.; Ryan, C. G.; Kirkham, R.; Moorhead, G.; Siddons, D. P. The X-ray fluorescence microscopy beamline at the Australian Synchrotron. *AIP Conf. Proc.* **2011**, *1365* (1), 219−222.
(38) Howard, D. L.; de Jonge, M. D.; Afshar, N.; Ryan, C. G.; Kirkham, R.; Reinhardt, J.; Kewish, C. M.; McKinlay, J.; Walsh, A.; Divitcos, J.; Basten, N.; Adamson, L.; Fiala, T.; Sammut, L.; Paterson, D. J. The XFM beamline at the Australian Synchrotron. *J. Synchrotron Radiat.* **2020**, *27* (5), 1447−1458.
(39) Kirkham, R.; Dunn, P. A.; Kuczewski, A. J.; Siddons, D. P.; Dodanwela, R.; Moorhead, G. F.; Ryan, C. G.; De Geronimo, G.; Beuttenmuller, R.; Pinelli, D.; Pfeffer, M.; Davey, P.; Jensen, M.; Paterson, D. J.; de Jonge, M. D.; Howard, D. L.; Küsel, M.; McKinlay, J. The Maia spectroscopy detector system: engineering for integrated pulse capture, low-latency scanning and real-time processing. *AIP Conf. Proc.* **2010**, *1234* (1), 240−243.
(40) Corzo Remigio, A.; Pošćić, F.; Nkrumah, P. N.; Edraki, M.; Spiers, K. M.; Brueckner, D.; van der Ent, A. Comprehensive insights in thallium ecophysiology in the hyperaccumulator *Biscutella laevigata*. *Sci. Total Environ.* **2022**, *838*, No. 155899.
(41) Jones, M. W. M.; Kopittke, P. M.; Casey, L.; Reinhardt, J.; Blamey, F. P. C.; van der Ent, A. Assessing radiation dose limits for X-ray fluorescence microscopy analysis of plant specimens. *Ann. Bot.* **2020**, *125* (4), 599−610.
(42) Krämer, U. Metal hyperaccumulation in plants. *Annu. Rev. Plant Biol.* **2010**, *61* (1), 517−534.
(43) Reeves, R. D.; Baker, A. J. M.; Jaffré, T.; Erskine, P. D.; Echevarria, G.; van der Ent, A. A global database for plants that

hyperaccumulate metal and metalloid trace elements. *New Phytol.* **2018**, *218* (2), 407−411.
(44) Kurz, H.; Schulz, R.; Römheld, V. Selection of cultivars to reduce the concentration of cadmium and thallium in food and fodder plants. *J. Plant Nutr. Soil Sci.* **1999**, *162* (3), 323−328.
(45) Liu, J.; Li, N.; Zhang, W.; Wei, X.; Tsang, D. C. W.; Sun, Y.; Luo, X.; Bao, Z. a.; Zheng, W.; Wang, J.; Xu, G.; Hou, L.; Chen, Y.; Feng, Y. Thallium contamination in farmlands and common vegetables in a pyrite mining city and potential health risks. *Environ. Pollut.* **2019**, *248*, 906−915.
(46) Fehlauer, T.; Collin, B.; Angeletti, B.; Santaella, C.; Dentant, C.; Chaurand, P.; Levard, C.; Gonneau, C.; Borschneck, D.; Rose, J. Uptake patterns of critical metals in alpine plant species growing in an unimpaired natural site. *Chemosphere* **2022**, *287*, No. 132315.
(47) Mizuno, N.; Takahashi, A.; Wagatsuma, T.; Mizuno, T.; Obata, H. Chemical composition of guttation fluid and leaves of *Petasites japonicus* v. *giganteus* and *Polygonum cuspidatum* growing on ultramafic soil. *Soil Sci. Plant Nutr.* **2002**, *48* (3), 451−453.
(48) Raschke, K. Stomatal action. *Ann. Rev, Plant Physiol.* **1975**, *26* (1), 309−340.
(49) Daniela, C.; Mirko, B.; Maria, P. A.; Costantina, F. L. M. Morpho-functional adaptations in *Cakile maritima* Scop. subsp. *maritima*: comparation of two different morphological types. *Caryologia* **2010**, *63* (4), 411−421.
(50) Vaněk, A.; Holubík, O.; Oborná, V.; Mihaljevič, M.; Trubač, J.; Ettler, V.; Pavlů, L.; Vokurková, P.; Penížek, V.; Zádorová, T.; Voegelin, A. Thallium stable isotope fractionation in white mustard: Implications for metal transfers and incorporation in plants. *J. Hazard. Mater.* **2019**, *369*, 521−527.
(51) Krasnodębska-Ostręga, B.; Sadowska, M.; Ostrowska, S. Thallium speciation in plant tissues—Tl(III) found in *Sinapis alba* L. grown in soil polluted with tailing sediment containing thallium minerals. *Talanta* **2012**, *93*, 326−329.
(52) Sadowska, M.; Biaduń, E.; Krasnodębska-Ostręga, B. Stability of Tl(III) in the context of speciation analysis of thallium in plants. *Chemosphere* **2016**, *144*, 1216−1223.
(53) Das, A. K.; Dutta, M.; Cervera, M. L.; de la Guardia, M. Determination of thallium in water samples. *Microchem. J.* **2007**, *86* (1), 2−8.
(54) Šamec, D.; Urlić, B.; Salopek-Sondi, B. Kale (*Brassica oleracea* var. *acephala*) as a superfood: review of the scientific evidence behind the statement. *Crit. Rev. Food Sci. Nutr.* **2019**, *59* (15), 2411−2422.
(55) FSANZ. *Food Standards Code Australia New Zealand- Schedule 19 - Maximum levels of contaminants and natural toxicants*. Australia New Zealand Food standards Code, Ed.; 2017.
(56) NHMRC. *Nutrient reference values for Australia and New Zealand including recommended dietary intakes*. National Health and Medical Research Council, New Zealand Ministry of Health, Ed.; Commonwealth of Australia: Canberra, 2006.
(57) Nepc, Z.; National Environment Protection Council (NEPC). *National Environement Protection (Assessment of Site Contamination) Measure 1999. Vol. 6: Schedue B5a*. Guideline on Ecological Risk Assessment Australian Government, Ed.; Canberra, 2013.
(58) Kim, Y.-H.; Ra, W.-J.; Cho, S.; Choi, S.; Soh, B.; Joo, Y.; Lee, K.-W. Method validation for determination of thallium by inductively coupled plasma mass spectrometry and monitoring of various foods in South Korea. *Molecules* **2021**, *26* (21), 6729.
(59) Canadian Council of Ministers of the Environment (CCME). *Canadian soil quality guidelines for the protection of environmental and human health: thallium*, Ed.; Environment Canada, Canadian Council of Ministers of the Environment: Winnipeg, 1999.
(60) Doulgeridou, A.; Amlund, H.; Sloth, J. J.; Hansen, M. National Food Institute - Technical University of Denmark. Review of Potentially Toxic Rare Earth Elements, Thallium and Tellurium in Plant-based Foods. *EFSA Journal* **2020**, *18* (S1), No. e181101.

https://doi.org/10.1021/acs.est.3c08113
Environ. Sci. Technol. 2024, 58, 2373−2383